Loss of *pdr-1/parkin* influences Mn homeostasis through altered *ferroportin* expression in *C. elegans*

Sudipta Chakraborty[a], **Pan Chen**[b], **Julia Bornhorst**[c], **Tanja Schwerdtle**[c], **Fabian Schumacher**[c,d], **Burkhard Kleuser**[c], **Aaron B. Bowman**[e], and **Michael Aschner**[b]

[a]Neuroscience Graduate Program, Vanderbilt University Medical Center, Nashville, TN, USA

[b]Department of Molecular Pharmacology, Albert Einstein College of Medicine, Bronx, NY

[c]Institute of Nutritional Sciences, University of Potsdam, Nuthetal, Germany

[d]Department of Molecular Biology, University of Duisburg-Essen, Essen, Germany

[e]Department of Neurology, Vanderbilt Kennedy Center, Center for Molecular Toxicology, Vanderbilt University Medical Center, Nashville, TN, USA

Abstract

Overexposure to the essential metal manganese (Mn) can result in an irreversible condition known as manganism that shares similar pathophysiology with Parkinson's disease (PD), including dopaminergic (DAergic) cell loss that leads to motor and cognitive impairments. However, the mechanisms behind this neurotoxicity and its relationship with PD remain unclear. Many genes confer risk for autosomal recessive, early-onset PD, including the *parkin/PARK2* gene that encodes for the E3 ubiquitin ligase Parkin. Using *Caenorhabditis elegans* (*C. elegans*) as an invertebrate model that conserves the DAergic system, we previously reported significantly increased Mn accumulation in *pdr-1/parkin* mutants compared to wildtype (WT) animals. For the current study, we hypothesize that this enhanced accumulation is due to alterations in Mn transport in the *pdr-1* mutants. While no change in mRNA expression of the major Mn importer proteins (*smf-1-3*) was found in *pdr-1* mutants, significant downregulation in mRNA levels of the putative Mn exporter ferroportin (*fpn-1.1*) was observed. Using a strain overexpressing *fpn-1.1* in worms lacking *pdr-1*, we show evidence for attenuation of several endpoints of Mn-induced toxicity, including survival, metal accumulation, mitochondrial copy number and DAergic integrity, compared to *pdr-1* mutants alone. These changes suggest a novel role of *pdr-1* in modulating Mn export through altered transporter expression, and provides further support of metal dyshomeostasis as a component of Parkinsonism pathophysiology.

Introduction

Parkinson's disease (PD) is the second most common neurodegenerative disorder, with a typical age of onset around 60 years of age[1]. This debilitating disease is characterized by

Corresponding Author: Michael Aschner, Forchheimer 209, 1300 Morris Park Avenue, Bronx, NY, Tel: 718.430.2317, Fax: 718.430.8922, Michael.Aschner@einstein.yu.edu.

selective dopaminergic (DAergic) cell loss in the substantia nigra pars compacta (SNpc) region of the brain. Hallmark symptoms of PD include bradykinesia, rigidity, tremors and postural instability that are often preceded by emotional instability and cognitive dysfunction. Unfortunately, PD is a progressive and irreversible condition[2]. Current treatments do not target the molecular origins of PD, warranting further examination into the mechanisms behind its pathophysiology.

Though PD is mostly idiopathic in its etiology, mutations in several genes have been connected to the disease[2]. For example, homozygous mutations in the *PARK2/parkin* gene are responsible for nearly 50% of an autosomal recessive, early-onset form of PD[3]. This gene encodes for an E3 ubiquitin ligase involved in the ubiquitin proteasome system (UPS) that targets substrates for degradation. Mutations in this gene result in impaired ligase activity and substrate binding that can lead to increased protein aggregation[4]. *Parkin* knockout animal models show a variety of PD-associated phenotypes, including hypokinetic deficits, DAergic cell loss and increased extracellular dopamine (DA) in the striatum[5, 6]. Parkin has also been more recently identified as a key regulator of mitophagy, an intracellular autophagic process designed to eliminate damaged mitochondria from the cell[7].

Despite the known genetic associations, familial cases often present with heterogeneity in their age-of-onset and symptomatology, in addition to nearly 90% of all PD cases manifesting without genetic disturbances[8]. The idiopathic component of the disease suggests a contribution of environmental risk factors in the development of PD. One such factor is the heavy metal manganese (Mn), an essential trace element found in many food sources consumed daily by humans. Mn serves as a necessary cofactor for enzymes involved in several critical processes, including reproduction, metabolism, development, and antioxidant responses[9]. While deficiency is a rare concern, the essentiality of Mn is mirrored by its neurotoxicity upon overexposure. Mn poisoning, or manganism, typically occurs from occupational exposures in industrial settings, such as in welding, where Mn-containing fumes and/or products are abundant[10, 11]. Mn is also found as an antiknock agent methylcyclopentadienyl manganese tricarbonyl (MMT) in gasoline, but limited studies currently exist on the impact of Mn release from combustion on general human health[12, 13]. Certain pesticides also contain Mn, making surface runoff from these agricultural uses an additional source of overexposure[1]. Moreover, Mn toxicity can also affect other susceptible populations, including ill neonates receiving total parenteral nutrition (TPN) that is supplemented with a trace element solution containing Mn. Intravenous TPN administration bypasses the gastrointestinal regulation of Mn absorption, resulting in 100% Mn retention[9]. Another population at risk of Mn poisoning includes patients suffering from hepatic encephalopathy and/or liver failure, as Mn is excreted from the body through the biliary system[14, 15]. On the other hand, individuals with iron (Fe) deficiency (e.g., iron deficiency anaemia), a highly prevalent nutritional condition, are at risk for increased Mn body burdens. As Mn shares similar transport mechanisms with Fe, higher Mn levels are often seen in conditions of low Fe levels[16].

Tight regulation through an intricate system of transport mechanisms helps maintain proper Mn homeostasis in cells. The divalent metal transporter 1 (DMT1) represents the primary mode of divalent Mn import[17]. However, Mn efflux remains less understood than Mn

import. We previously identified ferroportin (FPN), a well-known iron (Fe) exporter, as facilitating Mn export in cells and mice[18]. We have previously identified and characterized components of the Mn transport system in the *Caenorhabditis elegans* (*C. elegans*) model system. This nematode provides an attractive, alternative system that has a rapid life cycle, short lifespan, and large brood size. Additionally, the well-characterized genome allows for the utilization of various genetic mutants for studies. This nematode also conserves all necessary components of a fully functional DAergic system, allowing for the study of the effects of PD-associated genetic loss on the DAergic system. Our previous studies have identified SMF-1, SMF-2 and SMF-3 as the *C. elegans* homologs for DMT1, with SMF3 acting as the most DMT1-like homolog in its necessity to regulate Mn uptake[19]. Thus far, these proteins are the only known Mn importers in the worm. Furthermore, the worm contains 3 homologs for FPN: FPN-1.1, FPN-1.2 and FPN-1.3[20]. As of now, FPN-1.1 is the only known protein that conserves Fe efflux in *C. elegans*[21].

The overlap in sites of damage and similar symptomatology between manganism and Parkinsonism has warranted investigations into potential gene-environment interactions. For example, parkin has been shown to selectively protect against Mn-induced DAergic cell death *in vitro*[22], while rats exposed to Mn-containing welding fumes show increased Parkin protein levels[23]. Our previous study using *C. elegans* found significantly enhanced Mn accumulation in *pdr-1* (*parkin* homolog) knockout worms compared to WT worms[24]. With the aforementioned relationships between PD-associated genes and Mn toxicity, we hypothesized that this enhancement is due to an alteration in Mn homeostasis, at the level of transport, in the background of *pdr-1* loss. In the present study, while no significant change in mRNA expression of importers was seen, we found a downregulation of *fpn-1.1* mRNA. Upon overexpression of this exporter in *pdr-1* mutants, we found decreased metal levels that were associated with improved survival and DA-dependent behaviour. Together, our results provide further support for altered metal homeostasis as a component of the pathophysiology seen in Parkinsonism.

Experimental Procedures

Plasmid Constructs

Full-length wildtype (WT) *fpn-1.1* with C-terminal FLAG tag was PCR amplified using primers 5′-GGGGACAAGTTTGTACAAAAAAGCAGGCTACATGGCTTGGTTATCCGGAAAAG-3′ and 5′-GGGGACCACTTTGTACAAGAAAGCTGGGTTTCACTTGTCATCGTCGTCCTTGTAGTCTTCAAAAGTTGGCGAATCCAAC-3′ from cDNA library which was converted from total RNAs isolated from N2 worms (see below). The plasmid was created with Gateway recombinational cloning (Invitrogen). The above PCR product was initially recombined with the pDONR221 vector to create the pENTRY clone. Next, the *fpn-1.1* pENTRY construct was recombined into pDEST-*sur-5* vector[25], under the promoter of the acetoacetyl-coenzyme A synthetase (*sur-5*) gene. This plasmid was then used to create transgenic worms.

C. elegans Strains and Strain Construction

C. elegans strains were handled and maintained at 20°C as previously described[26]. Strains used were: N2, *wildtype* (*Caenorhabditis* Genetics Center, CGC) and VC1024, *pdr-1(gk448) III* (CGC). The MAB326 strain was created by microinjecting P$_{sur-5}$::*fpn-1.1* with pBCN27-R4R3 (P$_{rpl-28}$::PuroR, Addgene) and P$_{myo-3}$::mCherry (a gift from Dr. David Miller) into VC1024 strain. Over three stable lines were generated and analysed. Representative lines were selectively integrated by using gamma irradiation with an energy setting of 3600 rad.

Preparation of Manganese Chloride (MnCl$_2$)

2 M MnCl$_2$ (> 99.995% purity) (Sigma-Aldrich) stock solutions were prepared in 85 mM NaCl. To prevent oxidation, fresh working solutions were prepared shortly before each experiment. The range of concentrations used in all experiments are based on Mn dose-response curves recently published by our laboratory[24].

Mn-Induced Treatments and Lethality Assay

2500 synchronized L1 worms per group were acutely treated with MnCl$_2$ (0–100 mM) in siliconized tubes for 30 minutes. Worms were then pelleted by centrifugation at 7000 rpm for 3 minutes and washed four times with 85 mM NaCl. 30–50 worms were then pre-counted and transferred to OP50-seeded NGM plates in triplicate and blinded. 48 hours post-treatment, the total number of surviving worms was scored as a percentage of the original plated worm count.

TaqMan Gene Expression Assay

Total RNA was isolated via the Trizol method. Briefly, following Mn treatment, 1 mL of Trizol (Life Technologies) was added to each tube containing 20,000 worms resuspended in 100 μl 85 mM NaCl, followed by three cycles of freezing in liquid nitrogen and thawing at 37°C. 200 μL of chloroform was then added to each tube, followed by precipitation using isopropanol and washing with 75% ethanol. Following isolation, 1 μg total RNA was used for cDNA synthesis using the High Capacity cDNA Reverse Transcription Kit (Life Technologies), per manufacturer's instructions. cDNA samples were stored at 4°C. Quantitative real-time PCR (BioRad CFX96) was conducted in duplicate wells using TaqMan Gene Expression Assay probes (Life Technologies) for each gene, using the *gpd-3* (*gapdh* homolog) housekeeping gene for normalization after determining the fold difference using the comparative $2^{-\Delta Ct}$ method[27]. The following probes were used: *smf-1* (Assay ID: Ce02496635_g1); *smf-2* (Assay ID: Ce02496634_g1); *smf-3* (Assay ID: Ce02461545_g1); *fpn-1.1* (Assay ID: Ce02414545_m1); and *gpd-3* (Assay ID: Ce02616909_gH).

Metal Quantification

Total intraworm metal content was quantified using inductively coupled plasma mass spectrometry (ICP-MS), as previously described[24]. Briefly, 50,000 synchronized L1 worms were acutely treated with MnCl$_2$. Worms were then pelleted, washed five times with 85 mM NaCl and re-suspended in 1 mL 85 mM NaCl supplemented with 1% protease inhibitor. After sonication, an aliquot was taken for protein normalization using the bicinchoninic acid (BCA) assay kit (Thermo Scientific). Subsequently, the suspension was mixed again,

evaporated, and incubated with the ashing mixture (65% HNO_3/30% H_2O_2 (1/1) (both Merck)) at 95 °C for at least 12 h. After dilution of the ash with bidistilled water, metal levels were determined by ICP-MS.

Relative Mitochondrial DNA Copy Number Quantification

Relative mitochondrial DNA copy number was quantified using qPCR methods as previously described[28], with slight modifications. Briefly, 1,000 synchronized L1 worms were treated with $MnCl_2$ for 30 minutes, following by several washes. Total genomic DNA was then isolated using a 1X PCR buffer containing 0.1% Proteinase K, and subjected to the following lysis protocol in a thermal cycler (BioRad T100): 65°C for 90 minutes, 95°C for 15 minutes, and then hold at 4°C. Following lysis, DNA was diluted to 3 ng/µl, and real time PCR (BioRad CFX96) using SYBR Green (BioRad) was performed in triplicate with the following primers: *nd-1* for mtDNA (forward primer sequence: 5′-AGCGTCATTTATTGGGAAGAAGAC-3′; reverse primer sequence: 5′-AAGCTTGTGCTAATCCCATAAATGT-3′) and *cox-4* for nuclear DNA (forward primer sequence: 5′-GCCGACTGGAAGAACTTGTC-3′; reverse primer sequence: 5′-GCGGAGATCACC TTCCAGTA-3′). The PCR reaction consisted of: 2µL of template DNA, 1µL each of mtDNA and nucDNA primer pairs (400nM final concentration each), 12.5µL SYBR Green PCR Master Mix and 8.5µL H_2O. The following protocol was used: 50°C for 2 minutes, 95°C for 10 minutes, 40 cycles of 95°C for 15 seconds and 62°C for 60 seconds. The mitochondrial DNA content relative to nuclear DNA was calculated using the following equations: $C_T = (nucDNA \ C_T - mtDNA \ C_T)$, where relative mitochondrial DNA content = 2×2^{C_T}.

Glutathione Quantification

Total intracellular glutathione levels (reduced and oxidized GSH) have been determined using the "enzymatic recycling assay", as previously described[29]. Briefly, whole worm extracts were prepared out of 40,000 L1 worms acutely exposed to $MnCl_2$. This was followed by washes with 85 mM NaCl and sonication of the pellet in 0.12 mL ice-cold extraction buffer (1% Triton X-100, 0.6% sulfosalicylic acid) and 1% protease inhibitor in KPE buffer (0.1 M potassium phosphate buffer, 5 mM EDTA). After centrifugation at 10,000 rpm for 10 minutes at 4°C, the supernatant was collected, with an aliquot reserved for protein normalization using the BCA assay. Total intracellular GSH was quantified by measuring the change in absorbance per minute at 412 nm by a microplate reader (FLUOstar Optima microplate reader, BMG Labtechnologies) after reduction of 5,5′-dithio-2-nitrobenzoic acid (DTNB, Sigma-Aldrich). Hydrogen peroxide was used as a positive control.

Basal Slowing Response Assay

This assay of dopaminergic integrity was performed as previously described[30], with slight modifications. Briefly, 2500 synchronized L1 worms were acutely treated in siliconized tubes with $MnCl_2$ for 30 minutes. Following washes with 85 mM NaCl, treated worms were transferred to seeded NGM plates. 48 hours after treatment, 60 mm NGM plates with seeded with bacteria spread in a ring (inner diameter of ~1 cm and an outer diameter of ~3.5 cm) in

the center of the plate. Two seeded and two unseeded plates per group were kept at 37°C overnight, and allowed to cool to room temperature before use. Once Mn-treated animals reached the young adult stage, animals were washed at least two times with S basal buffer and then transferred to the central clear zone of the ring-shaped bacterial lawn (5–10 worms per plate) in a drop of S basal buffer that was delicately absorbed from the plate using a Kimwipe. After a five-minute acclimation period, the number of body bends in a 20-second interval was scored for each worm on the plate. Data are presented as the change ( ) in body bends per 20-second interval between worms transferred to unseeded plates and those with bacterial rings. Worms lacking *cat-2* (the homolog for tyrosine hydroxylase) were used as a positive control, as these worms are impaired in bacterial mechanosensation[30]. General locomotion was assessed using the number of body bends/20 seconds of the group transferred to unseeded plates.

Statistics

Dose-response lethality curves and all histograms were generated using GraphPad Prism (GraphPad Software Inc.). A sigmoidal dose-response model with a top constraint at 100% was used to draw the lethality curves and determine the respective LD_{50} values, followed by a one-way ANOVA with a Dunnett post-hoc test to compare all strains to their respective control strains. Two-way ANOVAs were performed on TaqMan gene expression, metal content, total GSH, relative mtDNA copy number and basal slowing response data, followed by Bonferroni's multiple comparison post-hoc tests.

Results

pdr-1 mutants show alterations in mRNA expression of Mn exporter-, but not importer-related genes

We previously reported a statistically significant increase in Mn accumulation in *pdr-1* mutants vs. WT worms[24]. To test whether this enhancement was due to a change in transcription of Mn importer and/or exporter genes, we performed quantitative reverse transcription PCR (qRT-PCR) to examine *smf-1,2,3* (Fig. 1A–1C) and *fpn-1.1* gene expression (Fig. 1D), respectively, following acute Mn exposure. Two-way ANOVA analysis showed no overall effect of Mn treatment on transcription of any of the genes tested. However, while *pdr-1* mutants showed no significant changes in *smf-1,2,3* (the importers) mRNA expression (Fig. 1A–1C), a significant genotype difference (p<0.0001) was noted in *fpn-1.1* (the exporter) between *pdr-1* mutants and WT animals. *Post-hoc* analysis revealed a significant *fpn-1.1* downregulation at 0 and 2.5 mM $MnCl_2$ (Fig 1D).

Overexpression of *fpn-1.1* in *pdr-1* mutants suppresses Mn-induced lethality

In addition to enhanced Mn accumulation, *pdr-1* mutants showed a leftward shift in the Mn dose-response survival curve, with WT worms exhibiting a LD_{50} of 10.43 mM[24]. To determine whether downregulation of *fpn-1.1* may have played a role in exacerbating Mn-induced lethality of *pdr-1* mutants, we overexpressed *fpn-1.1* in the *pdr-1* mutant background. Upon Mn exposure, *pdr-1* mutants overexpressing *fpn-1.1* (*pdr-1* KO; *fpn-1.1* OVR) exhibited a rightward shift in the dose-response curve of compared to *pdr-1* mutants alone (Fig. 2A). The LD_{50} of *pdr-1* KO; *fpn-1.1* OVR animals (10.84 mM) relatively

normalized to previously published WT levels, while *pdr-1* mutants alone show a LD_{50} of 7.416 mM (Table, 2B). Two-way ANOVA analysis showed a significant interaction effect (p=0.0064) between both genotype and treatment (p<0.0001).

Overexpression of *fpn-1.1* in *pdr-1* mutants decreases levels of pro-oxidant metals

Upon noting the improved survival in *pdr-1* KO; *fpn-1.1* OVR animals, we hypothesized that this attenuation in Mn-induced toxicity is associated with a decrease in redox active metal accumulation. Using inductively coupled plasma mass spectrometry (ICP-MS), we measured intraworm concentrations of various metals, including Mn, iron (Fe), zinc (Zn) and copper (Cu) following acute Mn exposure. To our surprise, Mn levels remained relatively similar between strains, though two-way ANOVA analysis revealed a significant treatment effect (p=0.0165). However, endogenous Fe levels were significantly decreased in *pdr-1* KO; *fpn-1.1* OVR animals compared to *pdr-1* KOs alone revealed as a significant genotype effect by ANOVA (Fig. 3B, p=0.0092). No significant changes were seen in Zn levels (Fig. 3C). However, similar to Fe, Cu levels were significantly decreased in *pdr-1* KO; *fpn-1.1* OVR animals compared to *pdr-1* KOs (Fig. 3D, p=0.0256), with no post-hoc level differences. In summary, Mn levels stayed relatively the same, while Fe and Cu were both significantly decreased in *pdr-1* KO; *fpn-1.1* OVR animals. These results indicate that the improved survival is probably due to decreased levels of Fe and Cu, and suggests that *fpn-1.1* may prefer Fe and Cu as substrates over Mn.

Overexpression of *fpn-1.1* in *pdr-1* mutants improves mitochondrial integrity and antioxidant response

Increased Mn levels in *pdr-1* KOs (*vs.* WT animals) have been noted concurrently with significantly increased basal levels of reactive oxygen species (ROS) and depleted basal levels of total glutathione (GSH)[24], suggesting an overall exacerbated environment of oxidative stress in *pdr-1* KO animals. Therefore, we next sought to determine whether the significant decrease in Fe and Cu levels (Fig. 3) and improvement in survival of *pdr-1* KO;*fpn-1.1* OVR animals (Fig. 2) were associated with improved defence mechanisms against oxidative stress. This was investigated using two measures: relative mitochondrial DNA (mtDNA) copy number and total GSH levels. Alterations in mtDNA copy number have been associated with aging and degenerative processes[30]. Moreover, parkin has been shown to regulate mitochondrial turnover to maintain proper mitochondrial integrity[7]. Using a quantitative PCR (qPCR) technique, we found *pdr-1* KO animals had a significantly elevated mtDNA copy number relative to WT animals, whereas *pdr-1* KO;*fpn-1.1* OVR animals exhibited levels similar to WT animals (Fig. 4A); two-way ANOVA analysis reveals a significant genotype effect (p=0.0116), though significance was not reached at the *post-hoc* level. Moreover, we previously published the basal depletion of total GSH in *pdr-1* KOs compared to WT controls. Given the reversal of increased mtDNA copy number in *pdr-1* KO;*fpn-1.1* OVR animals, we examined whether there was a similar rescue of GSH depletion. While statistical significance wasn't reached, there was a slight increase in GSH levels in *pdr-1* KO;*fpn-1.1* OVR animals relative to *pdr-1* KOs (Fig. 4C, p=0.09). In both measures, Mn treatment itself did not significantly affect the outcomes.

Overexpression of *fpn-1.1* in *pdr-1* mutants improves the DA-dependent basal slowing response

Loss of *parkin* is connected to PD-associated DAergic neurodegeneration, and we previously published similar results of *pdr-1* KOs showing increased DAergic neurodegeneration *vs.* WT worms with fluorescence microscopy[24]. Consequently, we investigated whether the visual effects of DAergic neurodegeneration persisted to alter a behavioral outcome of DAergic integrity. The basal slowing response is a DA-dependent behavior that affects the mechanosensation needed for proper food sensing in *C. elegans*, as worms slow their movement when encountering a bacterial lawn. Worms lacking *cat-2*, the homolog for tyrosine hydroxylase, are defective in this response from the loss of dopamine synthesis and do not slow down[31]. Thus, the changes ( ) in number of body bends between plates with and without bacteria reflect the integrity of DAergic neurons. Using this paradigm, *pdr-1* KO animals exhibited a significantly defective basal slowing response *vs.* WT animals (p<0.001) that was analogous to that of *cat-2* mutants (Fig. 5). The *pdr-1* KO;*fpn-1.1* OVR animals showed a partial rescue of the response, without reaching statistical significance. However, in the presence of Mn treatment, *pdr-1* KO;*fpn-1.1* OVR fully restored the response to WT levels, with the changes ( ) in number of body bends being significantly higher than *pdr-1* KOs alone (p<0.01). To ensure that these effects were not due to general locomotion differences, we compared the number of body bends per group on plates without bacterial lawns; there were no significant differences between all groups (data not shown).

Discussion

The relationship between genetic mutations and the contribution of environmental risk factors in the development of PD has yet to be clearly defined. In the present study, the *C. elegans* model system was utilized to investigate alterations in Mn homeostasis and toxicity in animals lacking *pdr-1/parkin*, a genetic risk factor for PD. We previously published evidence that animals lacking *pdr-1* show high sensitivity to an acute Mn exposure, with decreased survival and significantly elevated Mn accumulation compared to WT animals[24]. The present study aimed to determine whether the enhanced Mn concentrations were due to altered expression of Mn transporters in *C. elegans* to affect Mn homeostasis.

Parkin's role in regulating metal homeostasis has only recently begun to be investigated. Previous *in vitro* evidence has shown that parkin can modulate levels of the 1B isoform of DMT1 through ubiquitination[32]. Moreover, *Drosophila* studies show that both pharmacological (BCS/BPD) or genetic (increased expression of the metal responsive transcription factor 1, MTF-1) chelation of redox-active metals decreases oxidative stress, improves reduced lifespan and normalizes metal concentrations in *parkin* mutant flies[33, 34]. Therefore, parkin's regulation of metal homeostasis and its role as an E3 ligase raise the possibility of parkin-mediated regulation of Mn-responsive proteins. The *C. elegans* system represents a ideal model to study this possibility, as PDR-1 conserves its ligase activity[35], and their genome contains less E3 ligases[36] to minimize the possible compensatory mechanisms seen in vertebrate knockout models.

The enhanced Mn accumulation in *pdr-1* mutant animals may be a selective phenotype of this particular genetic background. Notably, our previous studies using methylmercury (MeHg) exposure do not show the same accumulation phenotypes in *pdr-1* KO's[37]. Moreover, Aboud *et al.* showed increased oxidative stress in response to Mn exposure in neuroprogenitor cells from patients possessing *parkin* mutations, despite exhibiting reduced Mn accumulation[38], which is opposite to our ICP-MS findings. This discrepancy may be due to their human data arising from isolated neuroprogenitors, whereas the current study assesses whole-worm Mn levels. Nonetheless, such studies provide further support of alterations in neuronal Mn biology in the presence of *parkin* mutations. This may be true for other PD genetic risk factors as well, as recent studies have highlighted the role of another PD-linked gene known as *PARK9*, which encodes for the P-type ATPase ion pump ATP13A2. Evidence shows that this protein modulates Zn homeostasis[39], with previous evidence indicating that this protein can also transport Mn[40]. However, our findings with the *pdr-1* mutant background show no differences in Zn accumulation, providing further support for a selective relationship between Parkin and Mn homeostasis.

Contrary to *in vitro* evidence of parkin-mediated control of a DMT isoform, we observed no significant changes in expression of the *smf* genes, especially with *smf-3* being the most DMT1-like homolog[19]. Instead, significant downregulation of *fpn-1.1* was observed in *pdr-1* KOs compared to WT animals. These findings suggest that the loss of *pdr-1* in *C. elegans* results in increased Mn accumulation from defective export, rather than from impaired uptake. Notably, we recently identified a novel role for SLC30A10 in Mn export that is associated with heightened risk for PD. However, no homologs for this protein are expressed in *C. elegans*[41]. Thus, for the present study, given the downregulation of *fpn-1.1* mRNA in *pdr-1* mutants, we investigated whether overexpression of the only known Mn exporter in *C. elegans* would result in a rescue of *pdr-1* mutant phenotypes.

Mn uptake is modulated by a variety of proteins, including: DMT1, the transferrin receptor (TfR), the choline transporter, the citrate transporter, the magnesium transporter HIP14, ATP13A2, the solute carrier 39 family of zinc transporters, and calcium channels[10]. Among these, DMT1 has been given the most attention, as it is not only the primary mode of uptake, but is also associated with parkinsonism. Increased DMT1 expression has been found in the SNpc of PD patients, as well as in SNpc of MPTP mouse models[42]. Elevated DMT1 mRNA expression and DAergic neurotoxicity was also seen in rats exposed to Mn-containing welding fumes[43]. Moreover, specific polymorphisms in DMT1 have been found in a Chinese population suffering from PD[44]. These studies highlight altered metal homeostasis in the etiology of Parkinsonism. Interestingly, the overexpression of FPN in our *pdr-1* mutants altered not only Mn, but Fe and Cu levels to a greater extent. We were not surprised to observe a treatment effect for Mn, as this was the only exogenous treatment administered to the nematodes. However, we did expect to see a greater decrease in Mn concentrations. It is possible that FPN's affinity for Fe is greater than that of Mn, as the differential binding affinities have yet to be determined. Moreover, as FPN has not been shown to export Cu, the decrease in Cu levels may be a secondary effect of lowered intracellular Fe due to increased Fe efflux. Fe-deficiency anaemia has been associated with copper deficiencies, though the mechanism remains unknown[45, 46]. Though future studies are needed to further elucidate

FPN's transport profile in *C. elegans*, the rescue of the *pdr-1* mutant phenotype through FPN overexpression supports our hypothesis that metal dyshomeostasis in the background of *pdr-1* loss may be due to alterations in transporter expression.

In addition to the well-characterized toxicity of Mn resulting in Parkinsonian symptoms, enhanced iron accumulation in the SN is often seen in PD brains[42, 47], with pharmacological Fe chelation showing potential therapeutic value[48, 49]. Moreover, Mn treatment has been recently shown to disrupt general metal homeostasis in WT *C. elegans*, with excess Mn resulting in altered Fe and Cu levels[50]. Though the authors of this study used slightly higher Mn concentrations (10–30 mM) than the present study, this was most likely due to the use of older worms treated for 24 hours, rather than larval stage worms acutely treated for 30 minutes. However, as their lowest dose (10 mM) is within the range of the doses used in the present study, similar findings were seen with higher Mn concentrations (30 mM) corresponding with comparatively lower Fe and Cu levels overall[50]. The results in the present study provide further support of the interplay between metals, as exogenous Mn treatment results in the alteration of endogenous metal concentrations that may alter vital downstream processes. It is possible that the combined effects of decreased Fe and Cu levels, rather than the moderate to slight decrease in Mn levels, results in the amelioration of the *pdr-1* KO phenotypes. Moreover, the connection between Cu and a mutant *parkin* background is further supported by recent human data showing increased Cu sensitivity in neuroprogenitors from patients carrying *PARK2* mutations[51].

The recently discovered role of parkin as a mediator of mitophagy has introduced the potential significance of mitochondrial integrity in Parkinsonism[52]; loss of *parkin* could result in the accumulation of defective mitochondria to increase cellular oxidative stress. This could explain the significant increase in relative mtDNA copy number in *pdr-1* KO animals as a measure that could equate with increased mitochondrial mass in *pdr-1* KOs. This data corresponds with our previously published findings that *pdr-1* KOs exhibit significantly increased ROS levels[24]. Notably, it seems controversial in the literature whether increased mtDNA copy number is protective or damaging in degenerative processes[53, 54]. However, increased mtDNA copy number has been associated with aging, as well as a response to increased oxidative stress[30]. Therefore, the increased copy number may also be in response to increased oxidative stress from enhanced Mn accumulation to compensate for damaged mitochondria. This may be especially true due to the preferential accumulation of Mn in mitochondria[55]. Consequently, the beneficial alterations in Mn, Fe and Cu in *pdr-1* KO;*fpn-1.1* OVR animals would then help to reverse this effect by decreasing metal-induced oxidative stress. Additionally, the increase in the antioxidant GSH in *pdr-1* KO;*fpn-1.1* OVR animals vs. *pdr-1* KO animals is modest, though it does not reach statistical significance. This may represent a slight improvement in the overall handling of oxidative stress. It has been previously shown that neurons treated with increasing Fe concentrations show depletion in GSH content[56]. This is similar to the elevation in GSH content of *pdr-1* KO;*fpn-1.1* OVR animals that also exhibit decreased Fe accumulation. However, we are limited in the present study, as we have been unsuccessful in using the microplate assay format to measure both GSSG and GSH. While *pdr-1* KO;*fpn-1.1* OVR and *pdr-1* KO animals show no difference in *gcs-1* (homolog for the glutamate-cysteine

ligase responsible for catalysing GSH synthesis) mRNA expression (data not shown), future studies should be done to determine whether this change in GSH is due to more reduced vs. oxidized forms of GSH.

Finally, we previously reported that *pdr-1* KO animals show an exacerbation of DAergic neurodegeneration compared to WT animals[24]. Currently, conflicting findings exist on the effects of Mn on DAergic neurodegeneration in *C. elegans*[50, 57]. However, this may be due to differences in treatment paradigms and doses. Additionally, fluorescence microscopy is a common technique to assess degeneration; however, microscopy for GFP visualization remains a mostly qualitative readout of cell death. Accordingly, we focused on an output parameter of an intact DAergic system by assaying a DA-dependent behavioural measure. The basal slowing response (BSR) is a well-known feeding response that requires DA and affects mechanosensation to properly recognize food sources (bacteria) in *C. elegans*[31]. Similar to our previous results[24], Mn treatment itself in WT animals did not result in a statistically significant decrease in BSR, though a slight decline was apparent. However, while *pdr-1* KOs show impairment in this response, the rescue of BSR deficits by *pdr-1* KO;*fpn-1.1* OVR animals normalizes to the WT response. These data suggest that the overexpression of FPN normalizes DAergic integrity in the background of *pdr-1* loss. The effect of Mn on BSR in *pdr-1* KO and *pdr-1* KO;*fpn-1.1* OVR animals is negligible. This may be due to the complete loss of *pdr-1* resulting in a "ceiling effect," such that the addition of Mn exposure does not further exacerbate the basal differences. However, the BSR in *pdr-1* KO;*fpn-1.1* OVR animals fully normalizes to WT levels upon treatment.

Notably, we cannot relate the improvement in BSR to the improved survival of *pdr-1* KO;*fpn-1.1* OVR animals, as it has been previously reported that ablation of DAergic neurons in nematodes does not affect overall survival[58]. However, the relationship between metals and dopamine toxicity is well known. Dopamine itself is a strong oxidant that can undergo an auto-oxidation process to produce highly damaging intermediates, which makes a strong argument for the vulnerability of DA-specific brain areas to toxins and other oxidants[59]. Mn has been shown to catalyse dopamine oxidation[60], while Fe has been shown to specifically bind neuromelanin found in DAergic neurons[61]. Thus, the *pdr-1* KO; *fpn-1.1* OVR animals may show improvement in the DA-dependent BSR due to the lower bioavailability of Mn, Fe and Cu that would otherwise participate in directly enhancing DA oxidation and/or indirectly producing damaging free radicals in an already susceptible cell type.

Conclusion

In conclusion, the present study provides further support for altered metal homeostasis as a critical component of PD pathophysiology. Using the genetically tractable *C. elegans* system, we show a novel role of *pdr-1/parkin* in modulating metal homeostasis following an acute Mn exposure, affecting metal efflux. Though human mutations in FPN have not yet been associated with PD, our findings demonstrate the importance and specificity of PD genetics (e.g. loss of *pdr-1/parkin*) in interacting with environmental factors to exacerbate physiological processes that may lead to cell death. Future studies should focus on potential therapeutic routes that help understand the interplay between *pdr-1/parkin*-mediated

mitochondrial dynamics and enhanced efflux of redox-active metals like Mn, Fe and Cu as a strategy against Mn-induced Parkinsonism.

Acknowledgments

References

1. ATSDR. US Department of Health and Human Services, Public Service. 2008

2. Lees AJ, Hardy J, Revesz T. Lancet. 2009; 373:2055–2066. [PubMed: 19524782]

3. Kitada T, Asakawa S, Hattori N, Matsumine H, Yamamura Y, Minoshima S, Yokochi M, Mizuno Y, Shimizu N. Nature. 1998; 392:605–608. [PubMed: 9560156]

4. Sriram SR, Li X, Ko HS, Chung KK, Wong E, Lim KL, Dawson VL, Dawson TM. Human molecular genetics. 2005; 14:2571–2586. [PubMed: 16049031]

5. Sang TK, Chang HY, Lawless GM, Ratnaparkhi A, Mee L, Ackerson LC, Maidment NT, Krantz DE, Jackson GR. The Journal of neuroscience: the official journal of the Society for Neuroscience. 2007; 27:981–992. [PubMed: 17267552]

6. Goldberg MS, Fleming SM, Palacino JJ, Cepeda C, Lam HA, Bhatnagar A, Meloni EG, Wu N, Ackerson LC, Klapstein GJ, Gajendiran M, Roth BL, Chesselet MF, Maidment NT, Levine MS, Shen J. The Journal of biological chemistry. 2003; 278:43628–43635. [PubMed: 12930822]

7. Vives-Bauza C, Zhou C, Huang Y, Cui M, de Vries RL, Kim J, May J, Tocilescu MA, Liu W, Ko HS, Magrane J, Moore DJ, Dawson VL, Grailhe R, Dawson TM, Li C, Tieu K, Przedborski S. Proceedings of the National Academy of Sciences of the United States of America. 2010; 107:378–383. [PubMed: 19966284]

8. Blesa J, Phani S, Jackson-Lewis V, Przedborski S. Journal of biomedicine & biotechnology. 2012; 2012:845618. [PubMed: 22536024]

9. Aschner JL, Aschner M. Molecular aspects of medicine. 2005; 26:353–362. [PubMed: 16099026]

10. Aschner M, Erikson KM, Herrero Hernandez E, Tjalkens R. Neuromolecular medicine. 2009; 11:252–266. [PubMed: 19657747]

11. Tuschl K, Mills PB, Clayton PT. International review of neurobiology. 2013; 110:277–312. [PubMed: 24209443]

12. Bhuie AK, Ogunseitan OA, White RR, Sain M, Roy DN. The Science of the total environment. 2005; 339:167–178. [PubMed: 15740767]

13. Finkelstein MM, Jerrett M. Environmental research. 2007; 104:420–432. [PubMed: 17445792]

14. Zeron HM, Rodriguez MR, Montes S, Castaneda CR. Journal of trace elements in medicine and biology: organ of the Society for Minerals and Trace Elements. 2011; 25:225–229.

15. Klos KJ, Ahlskog JE, Josephs KA, Fealey RD, Cowl CT, Kumar N. Archives of neurology. 2005; 62:1385–1390. [PubMed: 16157745]

16. Smith EA, Newland P, Bestwick KG, Ahmed N. Journal of trace elements in medicine and biology: organ of the Society for Minerals and Trace Elements. 2013; 27:65–69.

17. Garrick MD, Dolan KG, Horbinski C, Ghio AJ, Higgins D, Porubcin M, Moore EG, Hainsworth LN, Umbreit JN, Conrad ME, Feng L, Lis A, Roth JA, Singleton S, Garrick LM. Biometals: an international journal on the role of metal ions in biology, biochemistry, and medicine. 2003; 16:41–54.

18. Yin Z, Jiang H, Lee ES, Ni M, Erikson KM, Milatovic D, Bowman AB, Aschner M. Journal of neurochemistry. 2010; 112:1190–1198. [PubMed: 20002294]

19. Au C, Benedetto A, Anderson J, Labrousse A, Erikson K, Ewbank JJ, Aschner M. PloS one. 2009; 4:e7792. [PubMed: 19924247]

20. Anderson CP, Leibold EA. Frontiers in pharmacology. 2014; 5:113. [PubMed: 24904417]

21. De Domenico I, Lo E, Yang B, Korolnek T, Hamza I, Ward DM, Kaplan J. Cell metabolism. 2011; 14:635–646. [PubMed: 22019085]

22. Higashi Y, Asanuma M, Miyazaki I, Hattori N, Mizuno Y, Ogawa N. Journal of neurochemistry. 2004; 89:1490–1497. [PubMed: 15189352]

23. Sriram K, Lin GX, Jefferson AM, Roberts JR, Wirth O, Hayashi Y, Krajnak KM, Soukup JM, Ghio AJ, Reynolds SH, Castranova V, Munson AE, Antonini JM. FASEB journal: official publication of the Federation of American Societies for Experimental Biology. 2010; 24:4989–5002. [PubMed: 20798247]

24. Bornhorst J, Chakraborty S, Meyer S, Lohren H, Brinkhaus SG, Knight AL, Caldwell KA, Caldwell GA, Karst U, Schwerdtle T, Bowman A, Aschner M. Metallomics: integrated biometal science. 2014; 6:476–490. [PubMed: 24452053]

25. Leyva-Illades D, Chen P, Zogzas CE, Hutchens S, Mercado JM, Swaim CD, Morrisett RA, Bowman AB, Aschner M, Mukhopadhyay S. The Journal of Neuroscience. 2014; 34:14079–14095. [PubMed: 25319704]

26. Brenner S. Genetics. 1974; 77:71–94. [PubMed: 4366476]

27. Livak KJ, Schmittgen TD. Methods. 2001; 25:402–408. [PubMed: 11846609]

28. Hunter SE, Jung D, Di Giulio RT, Meyer JN. Methods. 2010; 51:444–451. [PubMed: 20123023]

29. Rahman I, Kode A, Biswas SK. Nature protocols. 2006; 1:3159–3165.

30. Lee HC, Yin PH, Lu CY, Chi CW, Wei YH. The Biochemical journal. 2000; 348(Pt 2):425–432. [PubMed: 10816438]

31. Sawin ER, Ranganathan R, Horvitz HR. Neuron. 2000; 26:619–631. [PubMed: 10896158]

32. Roth JA, Singleton S, Feng J, Garrick M, Paradkar PN. Journal of neurochemistry. 2010; 113:454–464. [PubMed: 20089134]

33. Saini N, Georgiev O, Schaffner W. Molecular and cellular biology. 2011; 31:2151–2161. [PubMed: 21383066]

34. Saini N, Oelhafen S, Hua H, Georgiev O, Schaffner W, Bueler H. Neurobiology of disease. 2010; 40:82–92. [PubMed: 20483372]

35. Springer W, Hoppe T, Schmidt E, Baumeister R. Human molecular genetics. 2005; 14:3407–3423. [PubMed: 16204351]

36. Papaevgeniou N, Chondrogianni N. Redox biology. 2014; 2:333–347. [PubMed: 24563851]

37. Martinez-Finley EJ, Chakraborty S, Slaughter JC, Aschner M. Neurochemical research. 2013; 38:1543–1552. [PubMed: 23609499]

38. Aboud AA, Tidball AM, Kumar KK, Neely MD, Ess KC, Erikson KM, Bowman AB. Neurotoxicology. 2012; 33:1443–1449. [PubMed: 23099318]

39. Kong SM, Chan BK, Park JS, Hill KJ, Aitken JB, Cottle L, Farghaian H, Cole AR, Lay PA, Sue CM, Cooper AA. Human molecular genetics. 2014; 23:2816–2833. [PubMed: 24603074]

40. Chesi A, Kilaru A, Fang X, Cooper AA, Gitler AD. PloS one. 2012; 7:e34178. [PubMed: 22457822]

41. Leyva-Illades D, Chen P, Zogzas CE, Hutchens S, Mercado JM, Swaim CD, Morrisett RA, Bowman AB, Aschner M, Mukhopadhyay S. The Journal of neuroscience: the official journal of the Society for Neuroscience. 2014; 34:14079–14095. [PubMed: 25319704]

42. Salazar J, Mena N, Hunot S, Prigent A, Alvarez-Fischer D, Arredondo M, Duyckaerts C, Sazdovitch V, Zhao L, Garrick LM, Nunez MT, Garrick MD, Raisman-Vozari R, Hirsch EC. Proceedings of the National Academy of Sciences of the United States of America. 2008; 105:18578–18583. [PubMed: 19011085]

43. Sriram K, Lin GX, Jefferson AM, Roberts JR, Chapman RS, Chen BT, Soukup JM, Ghio AJ, Antonini JM. Archives of toxicology. 2010; 84:521–540. [PubMed: 20224926]

44. He Q, Du T, Yu X, Xie A, Song N, Kang Q, Yu J, Tan L, Xie J, Jiang H. Neuroscience letters. 2011; 501:128–131. [PubMed: 21777657]

45. Prohaska JR, Broderius M. Biometals: an international journal on the role of metal ions in biology, biochemistry, and medicine. 2012; 25:633–642.

46. Prohaska JR. Annals of the New York Academy of Sciences. 2014; 1314:1–5. [PubMed: 24517364]

47. Ayton S, Lei P, Adlard PA, Volitakis I, Cherny RA, Bush AI, Finkelstein DI. Molecular neurodegeneration. 2014; 9:27. [PubMed: 25011704]

48. Mounsey RB, Teismann P. International journal of cell biology. 2012; 2012:983245. [PubMed: 22754573]

49. Ben-Shachar D, Eshel G, Riederer P, Youdim MB. Annals of neurology. 1992; 32(Suppl):S105–110. [PubMed: 1510367]

50. Angeli S, Barhydt T, Jacobs R, Killilea DW, Lithgow GJ, Andersen JK. Metallomics: integrated biometal science. 2014; 6:1816–1823. [PubMed: 25057947]

51. Aboud AA, Tidball AM, Kumar KK, Neely MD, Han B, Ess KC, Hong CC, Erikson KM, Hedera P, Bowman AB. Neurobiology of disease. 2014; 73C:204–212. [PubMed: 25315681]

52. de Vries RL, Przedborski S. Molecular and cellular neurosciences. 2013; 55:37–43. [PubMed: 22926193]

53. Podlesniy P, Figueiro-Silva J, Llado A, Antonell A, Sanchez-Valle R, Alcolea D, Lleo A, Molinuevo JL, Serra N, Trullas R. Annals of neurology. 2013; 74:655–668. [PubMed: 23794434]

54. Gu F, Chauhan V, Kaur K, Brown WT, LaFauci G, Wegiel J, Chauhan A. Translational psychiatry. 2013; 3:e299. [PubMed: 24002085]

55. Gavin CE, Gunter KK, Gunter TE. Neurotoxicology. 1999; 20:445–453. [PubMed: 10385903]

56. Aracena P, Aguirre P, Munoz P, Nunez MT. Biological research. 2006; 39:157–165. [PubMed: 16629175]

57. Benedetto A, Au C, Avila DS, Milatovic D, Aschner M. PLoS genetics. 2010; 6

58. Nass R, Hall DH, Miller DM 3rd, Blakely RD. Proceedings of the National Academy of Sciences of the United States of America. 2002; 99:3264–3269. [PubMed: 11867711]

59. Graumann R, Paris I, Martinez-Alvarado P, Rumanque P, Perez-Pastene C, Cardenas SP, Marin P, Diaz-Grez F, Caviedes R, Caviedes P, Segura-Aguilar J. Polish journal of pharmacology. 2002; 54:573–579. [PubMed: 12866711]

60. Garner CD, Nachtman JP. Chemico-biological interactions. 1989; 69:345–351. [PubMed: 2499426]

61. Bridelli MG, Tampellini D, Zecca L. FEBS letters. 1999; 457:18–22. [PubMed: 10486555]
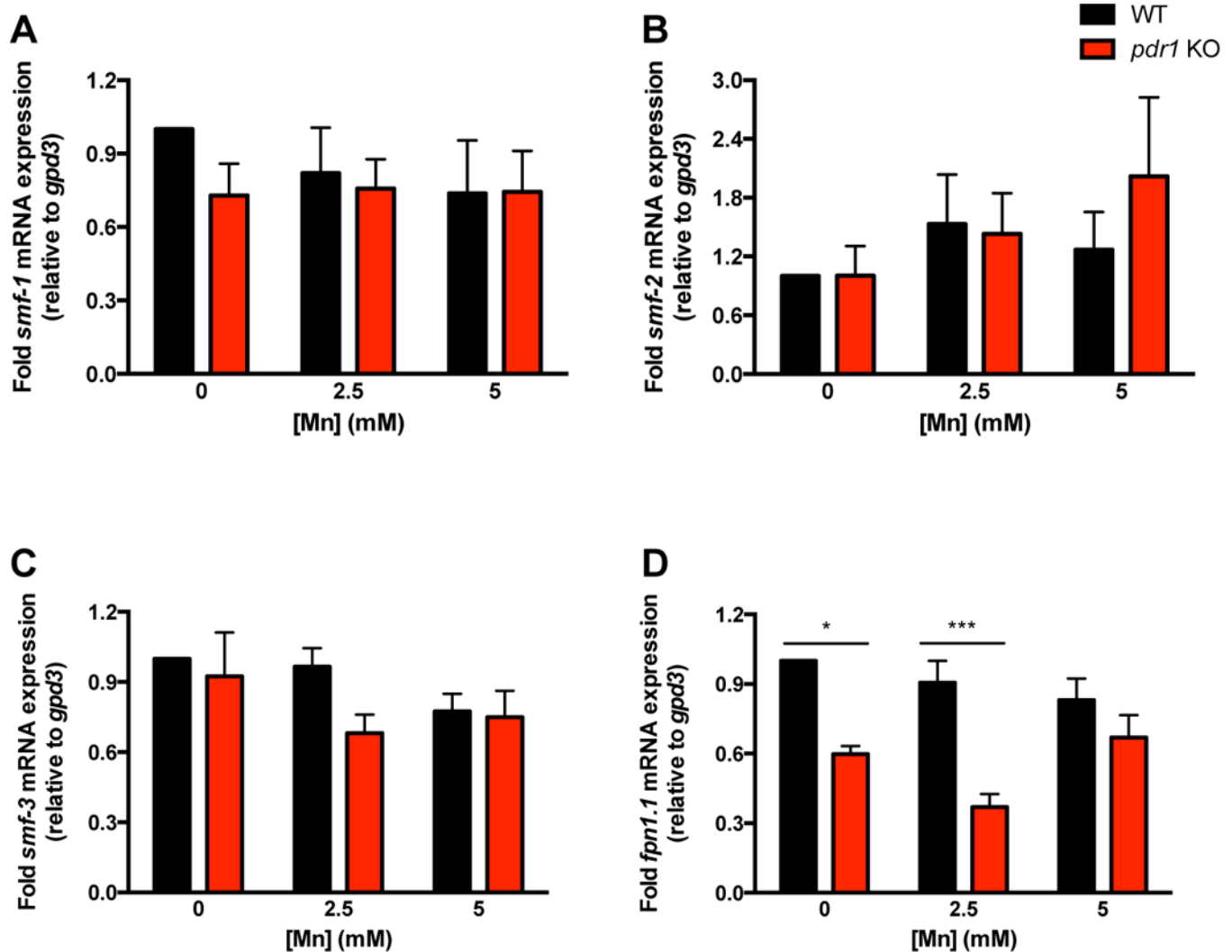
**Fig. 1. pdr-1 mutants show alterations in mRNA expression of Mn exporter, but not importer, genes**

(A-D) *smf-1,2,3 and fpn-1.1* mRNA expression after an acute, 30 min treatment of L1 worms with 0, 2.5 and 5 mM MnCl₂. Relative gene expression was determined by qRT-PCR. (A) *smf-1* mRNA expression in N2 (WT) and *pdr-1* KO animals. (B) *smf-2* mRNA expression in N2 (WT) and *pdr-1* KO animals. (C) *smf-3* mRNA expression in N2 (WT) and *pdr-1* KO animals. (D) *fpn-1.1* mRNA expression in N2 (WT) and *pdr-1* KO animals. (A-D) Data are expressed as mean values + SEM of at least five independent experiments in duplicates normalized to the untreated wildtype and relative to *gpd3* mRNA. Statistical analysis by two-way ANOVA: (A) interaction, ns; genotype, ns; concentration, ns; (B) interaction, ns; genotype, ns; concentration, ns; (C) interaction, ns; genotype, ns; concentration, ns; (D) interaction, ns (trend level, p=0.0639); genotype, p<0.0001; concentration, ns. *p < 0.05, ***p < 0.001 vs. respective wildtype worms.
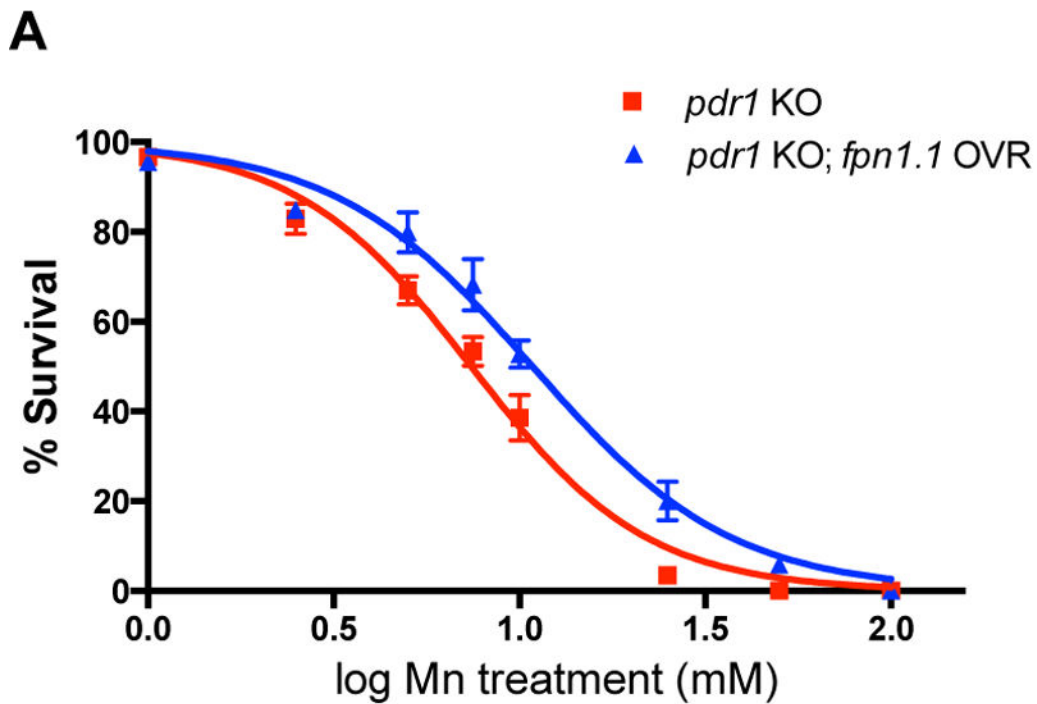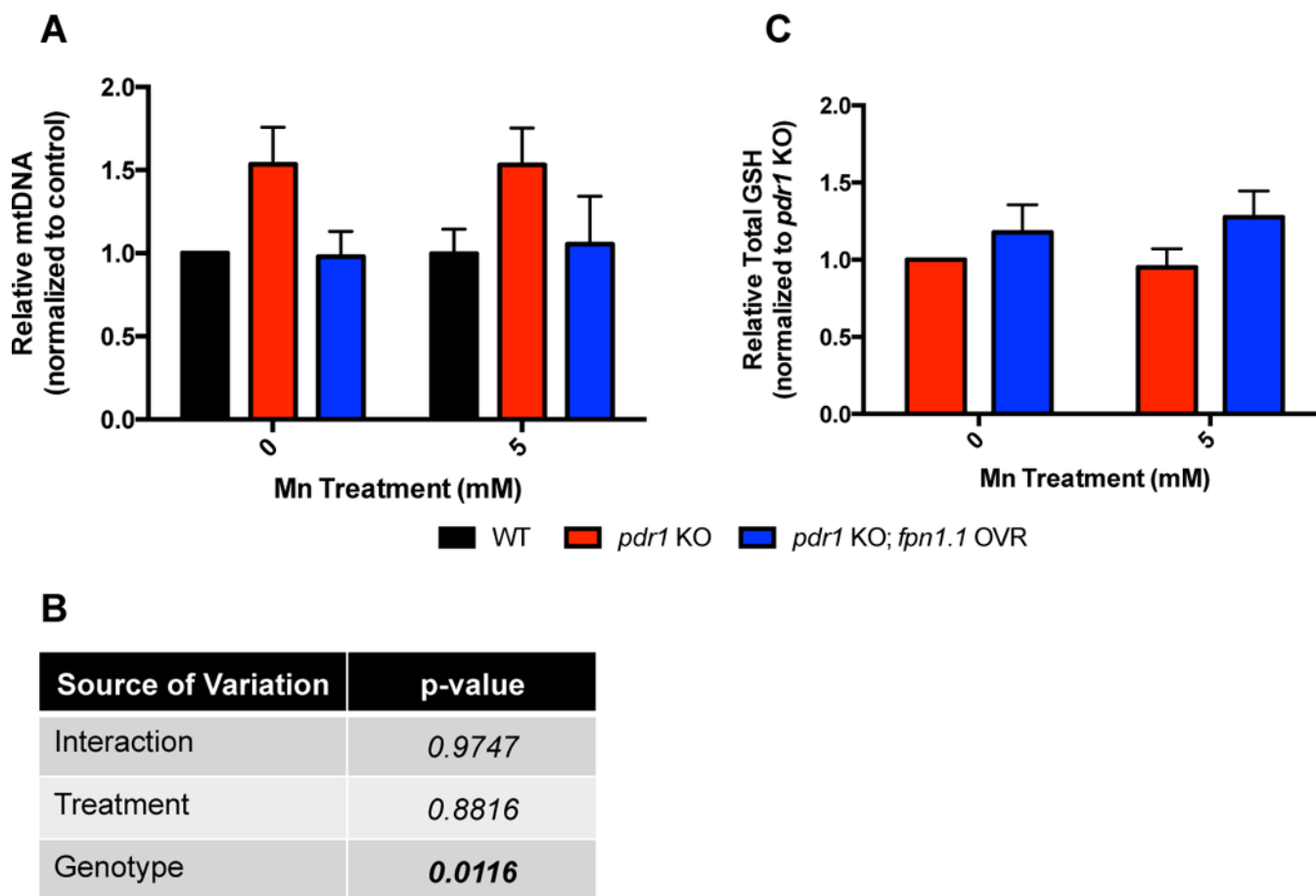
Fig. 2. Overexpression of fpn-1.1 in pdr-1 mutants rescues Mn-induced lethality
(A,B) Dose-response survival curves following acute Mn exposure. All values were compared to untreated worms set to 100% survival and plotted against the logarithmic scale of the used Mn concentrations. (A) *pdr-1* KO animals and *pdr-1* mutants overexpressing *fpn-1.1* (*pdr-1* KO; *fpn-1.1* OVR) were treated at the L1 stage for 30 min with increasing $MnCl_2$ concentrations. (B) The respective LD_{50} concentrations (mM $MnCl_2$) for both genotypes. Data are expressed as mean values + SEM from at least five independent experiments. Statistical analysis by two-way ANOVA: interaction, p=0.0064; genotype, p<0.0001; concentration, p<0.0001.
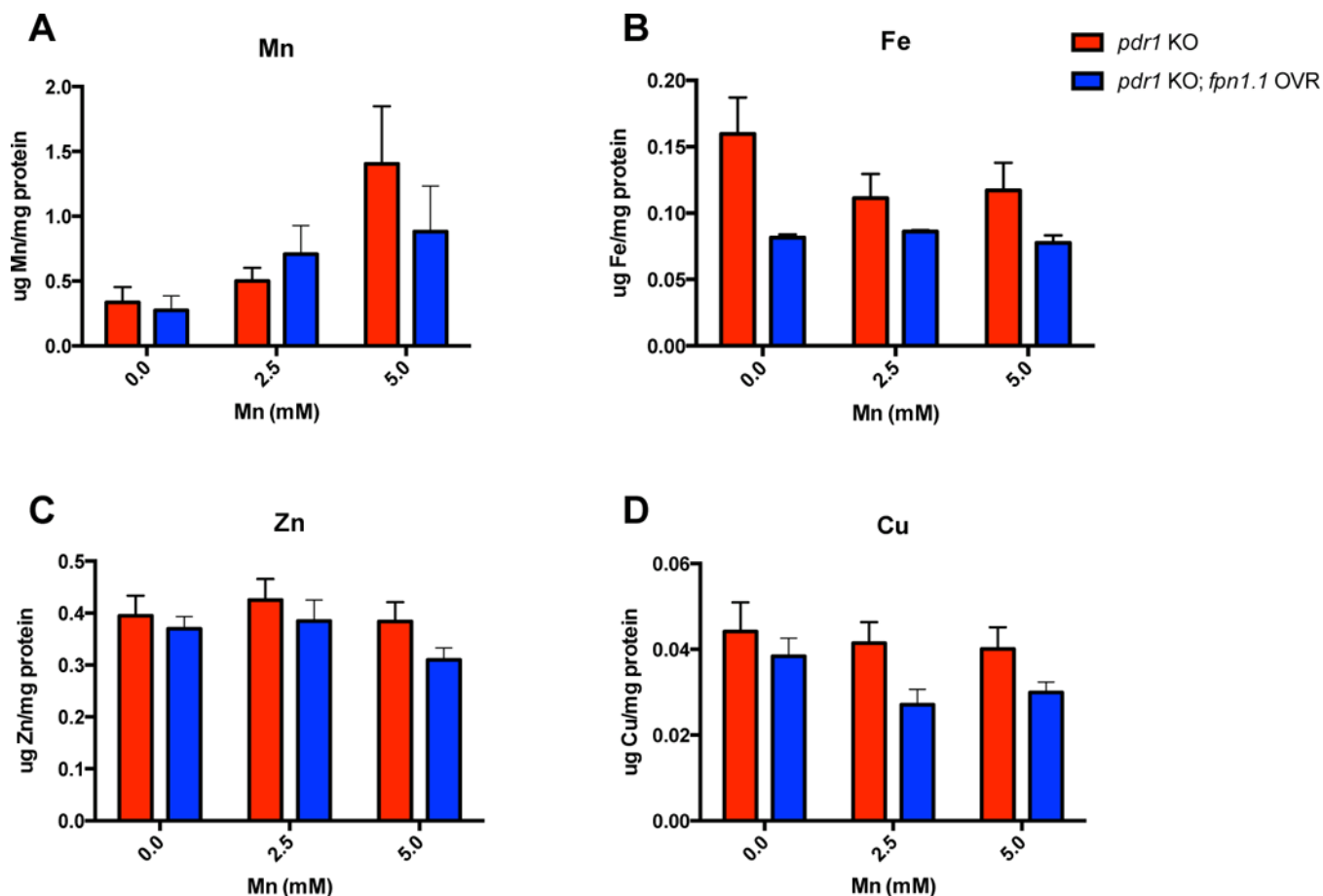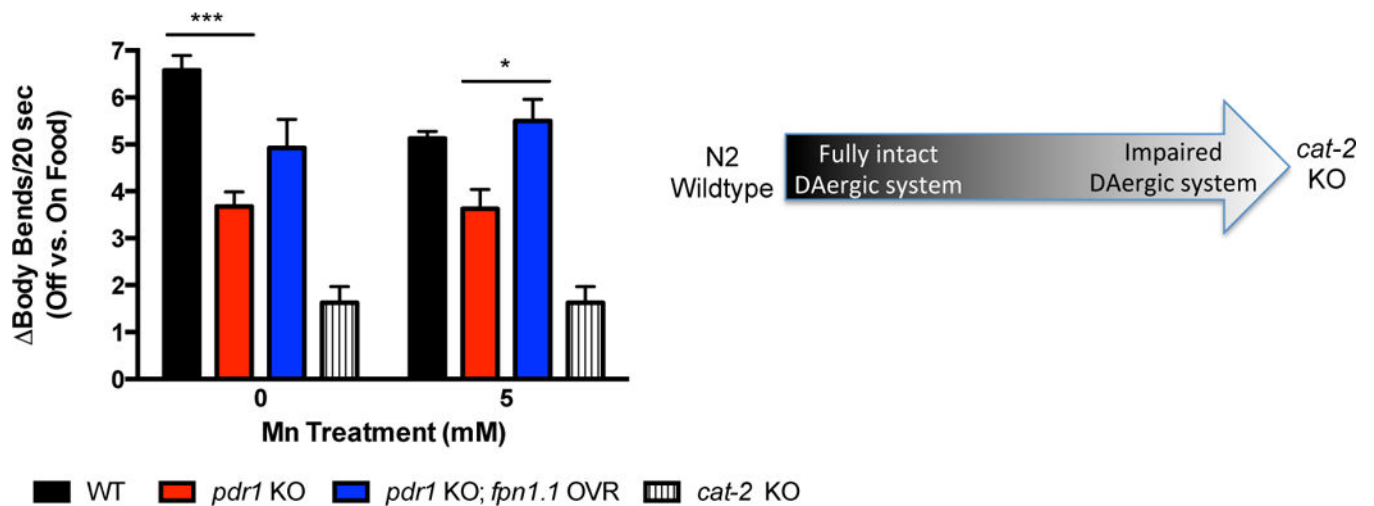
Fig. 3. Overexpression of fpn-1.1 in pdr-1 mutants decreases levels of highly pro-oxidant metals
(A-D) Intraworm metal concentrations following acute, 30 min $MnCl_2$ treatment (0, 2.5 and 5 mM) at the L1 stage, as quantified by ICP-MS/MS. (A) Mn content (μg Mn/mg protein) in *pdr-1* KO and *pdr-1* KO; *fpn-1.1* OVR animals. (B) Iron (Fe) content (μg Fe/mg protein) in *pdr-1* KO and *pdr-1* KO; *fpn-1.1* OVR animals. (C) Zinc (Zn) content (μg Zn/mg protein) in *pdr-1* KO and *pdr-1* KO; *fpn-1.1* OVR animals. (D) Copper (Cu) content (μg Cu/mg protein) in *pdr-1* KO and *pdr-1* KO; *fpn-1.1* OVR animals. (A-D) Data are expressed as mean values + SEM from at least six independent experiments and normalized to total protein content. Statistical analysis by two-way ANOVA: (A) interaction, ns; genotype, ns; concentration, $p=0.0165$; (B) interaction, ns; genotype, $p=0.0092$; concentration, ns; (C) interaction, ns; genotype, ns; concentration, ns; (D) interaction, ns; genotype, $p=0.0256$; concentration, ns.

Fig. 4. Overexpression of fpn-1.1 in pdr-1 mutants improves mitochondrial integrity and antioxidant response

(A) Relative mitochondrial DNA (mtDNA) copy number in *pdr-1* KO and *pdr-1* KO; *fpn-1.1* OVR animals following an acute, 30 min treatment with 0 and 5 mM MnCl$_2$. Relative gene expression was determined by qPCR. (B) Two-way ANOVA analysis of data in 4A showing genotype significance in mtDNA copy number. (C) Total glutathione (GSH) levels of *pdr-1* KO and *pdr-1* KO; *fpn-1.1* OVR animals following an acute, 30 min treatment with 0 and 5 mM MnCl$_2$. (A) Relative mtDNA copy number is expressed as a ratio of *nd-1* (mtDNA marker) to *cox-4* (nuclear DNA marker). Data are expressed as mean values + SEM of at least five independent experiments in duplicates normalized to the untreated N2 wildtype values. (C) Data are expressed as mean values + SEM of at least five independent experiments in duplicates, normalized to total protein content and relative to untreated *pdr-1* KO values. Statistical analysis by two-way ANOVA: (A) interaction, ns; genotype, p=0.0116; concentration, ns; (B) interaction, ns; genotype, ns (trend level, p=0.09); concentration, ns.

Fig. 5. Overexpression of fpn-1.1 in pdr-1 mutants improves the DA-dependent basal slowing response

Behavioral data are expressed as the change ( ) in body bends per 20 seconds between treated (5 mM $MnCl_2$) and untreated WT, *pdr-1* KO and *pdr-1* KO; *fpn-1.1* OVR animals placed on plates without food vs. plates with food. Schematic shows the spectrum of change, with N2 wildtype animals possessing a higher change in body bends (i.e., a fully intact DAergic system) to *cat-2* mutants possessing a smaller, almost negligible change in body bends (i.e., an impaired DAergic system). *cat-2* KO animals were used as a positive control. Statistical analysis by two-way ANOVA: interaction, ns (trend level, $p=0.0872$); genotype, $p<0.0001$; concentration, ns. ***$p<0.001$ vs. untreated WT, *$p<0.05$ vs. *pdr-1* KO.